



## Review

Dielectric properties of soft chemical method derived  $\text{CaCu}_3\text{Ti}_4\text{O}_{12}$  thin films onto Pt/TiO<sub>2</sub>/Si(1 0 0) substratesF. Moura<sup>c,1</sup>, E.C. Aguiar<sup>a,2</sup>, E. Longo<sup>a,2</sup>, J.A. Varela<sup>a,2</sup>, A.Z. Simões<sup>b,\*</sup><sup>a</sup> Laboratório Interdisciplinar em Cerâmica, Instituto de Química, Universidade Estadual Paulista, P.O. Box 355, 14801-907 Araraquara, São Paulo, Brazil<sup>b</sup> Universidade Estadual Paulista (Unesp) – Faculdade de Engenharia de Guaratinguetá, Av. Dr Ariberto Pereira da Cunha 333, Bairro Pedregulho, P.O. Box 355, 12.516-410 São Paulo, Brazil<sup>c</sup> Universidade Federal de Itajubá (Unifei) – Campus Itabira, Rua São Paulo 377, Bairro Amazonas, P.O. Box 355, 35900-37 Itabira, Minas Gerais, Brazil

## ARTICLE INFO

## Article history:

Received 17 November 2010

Received in revised form

23 December 2010

Accepted 24 December 2010

Available online 31 December 2010

## Keywords:

Thin films

Dielectrics

Chemical synthesis

X-ray diffraction

## ABSTRACT

Calcium copper titanate,  $\text{CaCu}_3\text{Ti}_4\text{O}_{12}$  (CCTO), thin film has been deposited by the soft chemical method on Pt/Ti/SiO<sub>2</sub>/Si (1 0 0) substrates at 700 °C for 2 h. The peaks were indexed as cubic phase belonging to the  $Im\bar{3}$  space group. The film exhibited a duplex microstructure consisting of large grains of 130 nm in length and regions of fine grains (less than 80 nm). The CCTO film capacitor showed a dielectric loss of 0.031 and a dielectric permittivity of 1020 at 1 MHz. The  $J$ – $V$  behavior is completely symmetrical, regardless of whether the conduction is limited by interfacial barriers or by bulk-like mechanisms. Based on impedance analyses, the equivalent circuit of CCTO film consisting of a resistor connected in series with two resistor–capacitor (RC) elements.

© 2011 Elsevier B.V. All rights reserved.

## Contents

1. Introduction .....	3817
2. Experimental procedures .....	3818
3. Results and discussion .....	3818
4. Conclusions .....	3821
Acknowledgments .....	3821
References .....	3821

## 1. Introduction

The recent observation by Subramanian et al. [1] of a giant dielectric constant in calcium copper titanate,  $\text{CaCu}_3\text{Ti}_4\text{O}_{12}$  (CCTO), has led to considerable efforts aimed to understand the origin of this behavior. The high frequency dielectric constant of about  $10^4$ – $10^5$  is practically frequency independent between DC and  $10^6$  Hz and possesses good temperature stability over a range from 100 to 400 K [2–5]. CCTO shows an  $Im\bar{3}$  space group [1,5], derived from the ideal cubic perovskite structure by superimposing a body centered ordering of Ca and Cu ions and a pronounced tilting of the titanium centered octahedra. This tilting alters the coordination

of Ca and Cu cations, leading to a square-planar environment for Cu and 12-coordinate icosahedral for Ca. The Cu–O distances show no variation with temperature (in the range 50–300 K), due to the high rigidity of these bonds [6]. Although the large number of works published about this material, there is still no commonly accepted model explaining the obtained values of dielectric constant ( $\epsilon$ ) shown by CCTO, mainly due to the discrepancy of the obtained results even for materials prepared in a similar way. Some authors propose intrinsic defects, such as stoichiometry variations [7], oxygen vacancies, presence of twinings [8] or aliovalences of Ti and Cu ions [9], as the source of the observed values of  $\epsilon$ . These defects should be inherent to the material, though the preparation process can affect their quantity or even nature. On the other hand, some other authors propose the presence of secondary phases that form layered structures giving rise to an enhancement of the material's dielectric constant, as stated out by the internal barrier layer

\* Corresponding author. Tel.: +55 12 3123 2765.

E-mail address: [alezipo@yahoo.com](mailto:alezipo@yahoo.com) (A.Z. Simões).<sup>1</sup> Tel.: +55 31 3834 6472.<sup>2</sup> Tel.: +55 16 3301 6643.

capacitance (IBLC) model [10]. This model is commonly accepted for ceramic samples and also on thin films [11]. In the case of single crystals the presence of such layered structures is highly controversial, although it has been recently proposed that defect structures form layers that give rise to an IBLC-like effect [12]. The nature of the proposed barriers has still not been fully characterised. Most authors associate them to the intergranular material [13], although some other structures, as intrinsic twin boundaries, have also been proposed [8]. The intergranular layers are composed mainly of Cu oxides, with small amounts of Ti and Ca oxides [14]. This Cu-oxide rich phase forms a liquid at the sintering temperature, being an important factor for the growth of the CCTO grains, which is mediated by the presence of the liquid phase. It has been demonstrated that the intergranular phase shows a higher resistivity than the grains interior [15].

Most of the works have been reported on the preparation of CCTO thin films based on physical deposition techniques as pulsed-laser deposition (PLD) [16–18]. Scarce works report the use of chemical solution deposition methods (CSD) for the thin film preparation [19,20]. Among various methods such as metal–organic chemical vapour deposition, pulsed laser deposition and sol–gel, the soft chemical method has its advantages over the other production techniques include its low cost, good compositional homogeneity, relatively low processing temperatures and the ability to coat large substrate areas [21,22]. In this paper, we report the growth and dielectric characterization of CCTO thin films deposited on Pt/TiO<sub>2</sub>/SiO<sub>2</sub>/Si substrates by the soft chemical method without any buffer layer.

## 2. Experimental procedures

The precursor solutions of calcium, copper and titanium were prepared by adding the raw materials to ethylene glycol and concentrated aqueous citric acid under heating and stirring. Appropriate quantities of solutions of Ca, Cu and Ti were mixed and homogenized by stirring at 90 °C. The molar ratio of metal:citric acid:ethylene glycol was 1:4:16. The viscosity of the resulting solution was adjusted to 20 cp by controlling the water content using a Brookfield viscosimeter. Details of the precursor method has been described in detail elsewhere [23]. The films were deposited at Pt(1 0 0)/Ti/SiO<sub>2</sub> substrates by spinning the deposition solution at 5000 rpm for 30 s. After deposition, the films were treated at 350 °C for 2 h to decompose the organic material. The film thickness was reached by repeating 10 times the spin-coating and heating treatment cycles. Finally, the films were crystallized at 700 °C for 2 h in ambient atmosphere.

After crystallization, the films were characterized by X-ray diffraction (XRD; Rigaku-DMAX 2500PC) at 40 kV and 150 mA from 2 $\theta$  (20–80) following the phase evolution. The thickness of the annealed films was determined by scanning electron microscopy (Topcom SM-300) at the transverse section evaluating the back-scattering electrons. The film annealed at a static atmosphere is 250 nm thick. Raman measurements were performed using an ISA T 64000 triple monochromator. An optical microscope with 80 $\times$  objective was used to focus the 514.5-nm radiation from a Coherent Innova 99 Ar<sup>+</sup> laser on the sample. The same microscope was used to collect the back-scattered radiation. The scattering light dispersed was detected by a charge-coupled device (CCD) detection system = 0.3 mm. Infrared analysis was performed on (Bruker–Equinox 55, Germany) Fourier Transformed Infrared spectrometer (FT-IR), using a 30° specular reflectance accessory. FT-IR reflectance spectra of the films were recorded at room temperature in the 400–1200 cm<sup>-1</sup> range. Top Pt electrodes (0.5 mm diameter) were prepared for the electrical measurements by evaporation through a shadow mask at room temperature. The leakage current–voltage (*J*–*V*) characteristic was determined with a voltage source measuring unit (Radiant Technology 6000 A). The relative dielectric constant  $\epsilon_r$  and the dissipation factor  $\tan \delta$  were measured versus frequency using an impedance analyser (model 4192 A, Hewlett Packard). Impedance measurements were performed with a frequency response analyser (HP 4192) with amplitude of 100 mV. All measurements were conducted at room temperature.

## 3. Results and discussion

Fig. 1 shows a typical  $\theta$ –2 $\theta$  X-ray diffraction scan of the as prepared CCTO thin film deposited on Pt/Ti/SiO<sub>2</sub>/Si substrate and annealed at 700 °C for 2 h. The film is fully crystallized since intense peaks are evident. The presented composition is a single-phase cubic copper calcium titanate belonging to the *Im*–3 space group

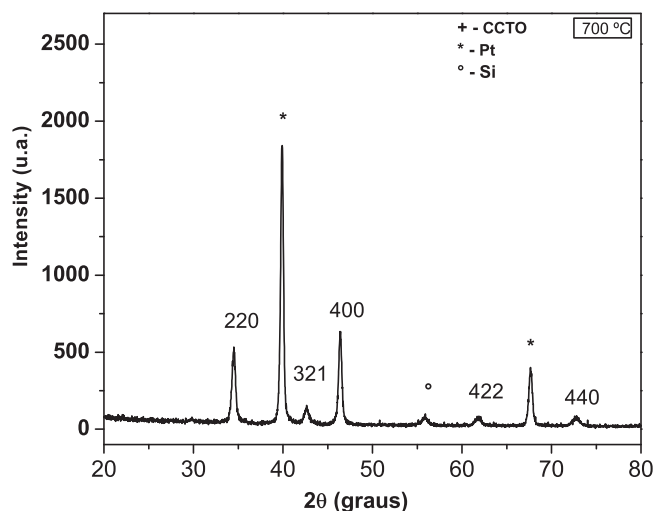


Fig. 1. X-ray diffraction data for CCTO thin film deposited by the soft chemical method at 700 °C for 2 h in ambient atmosphere.

(75–1149), whose planes are indexed in Fig. 1. Besides CCTO peaks, the characteristic peak for (1 1 1) platinum coated silicon substrates at 2 $\theta$  = 40° was identified. Compared with the XRD intensity from the substrate, the XRD reflections from CCTO are obviously smaller. This is mainly due to the polycrystalline character as well as the relatively small thickness of the CCTO film.

The FT-IR reflection spectra of the CCTO thin film annealed at 700 °C for 2 h is shown in Fig. 2. The lattice vibration of the films was analyzed. A broad reflection band of the BO<sub>6</sub> stretching mode was observed at 600–840 cm<sup>-1</sup> suggesting the formation of perovskite phase [24,25]. The reflection band at 786 cm<sup>-1</sup> indicates good crystallization of CCTO film and can be considered a network stiffening and a structural rearrangement, due the antiresonance with the longitudinal optic (LO) phonon modes. TiO<sub>6</sub> units are anticipated to exhibit six normal vibrational bands, but only  $\nu_{d}^{as}$  (F) and  $\delta_d$  (F) modes were reported to be active in the FT-IR spectrum. In the FT-IR spectrum of the CCTO film besides the peak related to formation of perovskite phase, one additional prominent band was also observed at 552 cm<sup>-1</sup>. Based up on the literature survey, this band is identified due to Ti–O–Ti symmetric stretching vibrations of TiO<sub>6</sub> structural units (600 cm<sup>-1</sup>) [26–28]. However, in our work the band

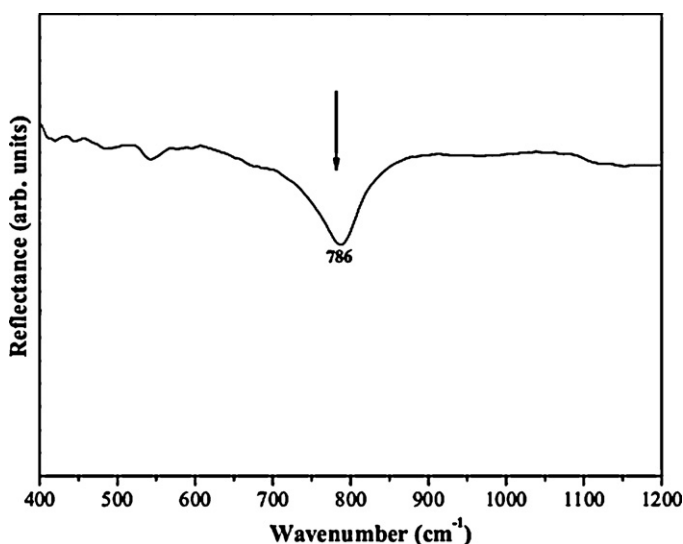
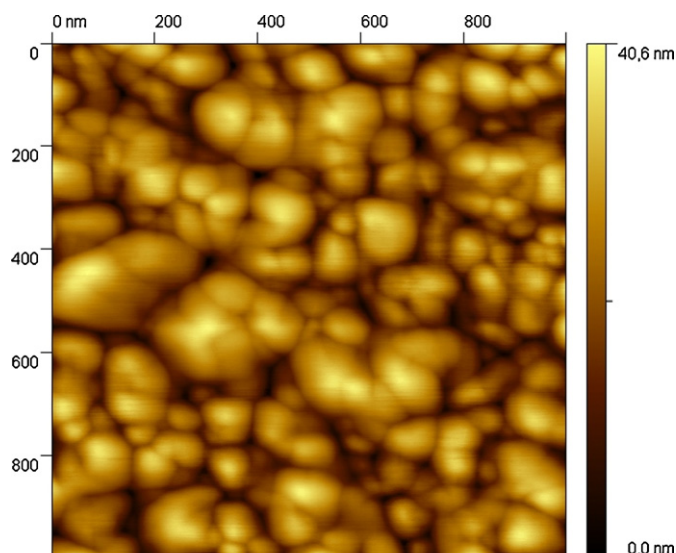


Fig. 2. Infrared spectra for CCTO thin film deposited by the soft chemical method at 700 °C for 2 h in ambient atmosphere.



**Fig. 3.** Atomic force microscopy for CCTO thin film deposited by the soft chemical method at 700 °C for 2 h in ambient atmosphere.

due to  $\text{TiO}_6$  structural units has exhibited a shift gradually towards higher wavenumber due the strain caused by differences in lattice parameters and thermal expansion coefficients between CCTO and Pt substrate.

The surface morphology of the CCTO thin film was also observed by AFM measurements (Fig. 3). CCTO film exhibited homogeneous microstructure consisting of small and large grains with a statistical roughness, root mean square (RMS) of 4.2 nm approximately. The single layer CCTO film formed on Pt/Ti/SiO<sub>2</sub>/Si substrates was found to be effective in improving the surface morphology of synthesized film, because the precursor film underwent the optimized nucleation and growth process producing films with a homogeneous and dense microstructure. Also, the homogeneous microstructure of CCTO film may affect the leakage properties, because the voltage can be applied uniformly onto it. The AFM surface image supports the XRD results revealing the polycrystalline nature. The film exhibited a duplex microstructure consisting of large grains of 130 nm in length and regions of fine grains (less than 80 nm). The grain growth in some regions might be attributed to the presence of CuO based liquid phase sintering [14].

Fig. 4 shows the Raman spectra of the CCTO film crystallized at 700 °C for 2 h in ambient conditions. Raman spectra in the CCTO thin film show the order–disorder degree of the atomic structure at short range. The modes further split into longitudinal and transverse components due the long electrostatic forces associated with lattice ionicity. There, we can easily find the main peaks at 143 cm<sup>-1</sup>, 296 cm<sup>-1</sup>, 346 cm<sup>-1</sup>, 445 cm<sup>-1</sup>, 506 cm<sup>-1</sup> and 623 cm<sup>-1</sup>, which are in agreement with other reported results for CCTO [29]. The Raman line at 296 cm<sup>-1</sup> is almost certainly associated with the Eg mode [30]. 445 cm<sup>-1</sup> and 506 cm<sup>-1</sup> peaks are associated with the Ag symmetry ( $\text{TiO}_6$ ) rotation-like. These rotation movements of the  $\text{TiO}_6$  octahedra would be highly influenced by the presence of Cu atoms on the lattice, since Cu–O bonds are very rigid and should impede the rotation of the octahedrons. The reduction of the rotation modes intensity should then be associated to the observed incorporation of Cu into the crystal lattice. However, we can detect other peaks, which are not predictable by the CCTO structural models [31]: 143 cm<sup>-1</sup> and 623 cm<sup>-1</sup>. These lines can be associated to the Raman active normal modes of the small minority phases  $\text{TiO}_2$  (anatase phase) and CuO [32,33], respectively located at the grain boundary. The Raman band assigned to  $\text{TiO}_6$  structural units seems to be merged with symmetric stretching vibration of Cu–O–Cu band

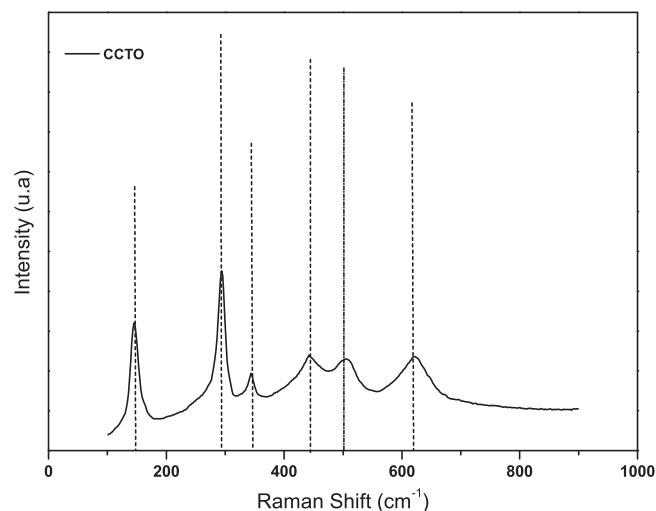


**Fig. 4.** Raman spectra for CCTO thin film deposited by the soft chemical method at 700 °C for 2 h in ambient atmosphere.

indicating possible linkages of the type Cu–O–Ti, in the network [34]. The Raman spectral studies clearly indicated no presence of  $\text{TiO}_4$  structural units in the CCTO film [35]. The absence of the band due to  $\text{TiO}_4$  structural units observed in the Raman spectrum of the CCTO film indicates, the presence of titanium ions largely in tetragonal positions, occupy substitutional positions. Due the high annealing temperature of the CCTO film, the intensity of the band due to  $\text{TiO}_6$  structural units is observed to increase at the expense of the band due to  $\text{TiO}_4$  structural units, indicating an increasing degree of order in the dielectric film.

Low leakage current density is another important consideration for memory device applications. A typical leakage current characteristic for CCTO thin film is given in Fig. 5. The curve was recorded with a voltage step width of 0.1 V and elapsed time of 1.0 s for each voltage, here the measured logarithmic current density ( $\log J$ ) versus the voltage (V) is shown. It can be seen that there are two clearly different regions. The current density increases linearly with the external electric field in the region of low electric field strengths, suggesting an ohmic conduction. This ohmic behavior occurs in insulating film as long as the film is quase neutral, that is, as long as the bulk generated current in the film exceeds the current due to injected free carriers from the electrode. This current would be due to the hopping conduction mechanism in a low electric field, because thermal excitations of trapped electrons

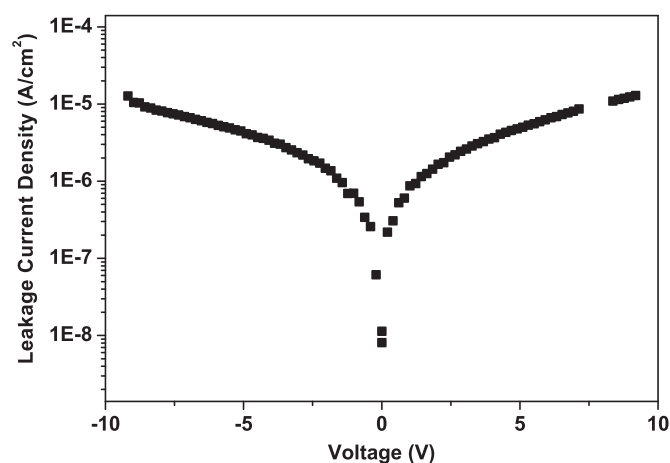


**Fig. 5.** Leakage current density versus voltage for CCTO thin film deposited by the soft chemical method at 700 °C for 2 h in ambient atmosphere.

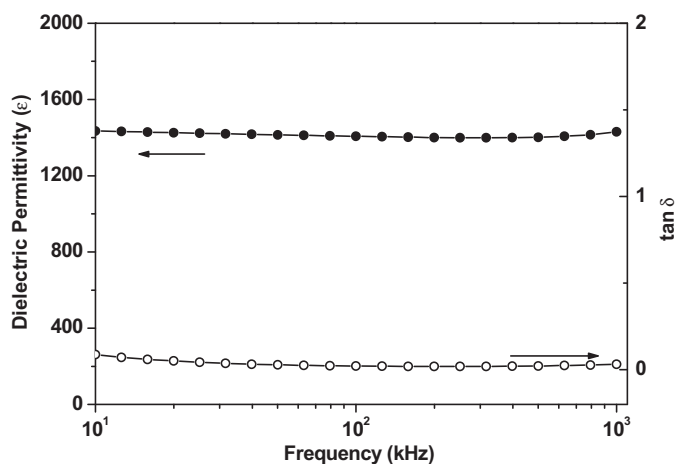


Fig. 6. Dielectric permittivity and dielectric loss for CCTO thin film deposited by the soft chemical method at 700 °C for 2 h in ambient atmosphere.

from one trap site to another dominate the transport in the films. At higher field strengths the current density increases exponentially, which implies that at least one part of the conductivity results from Schottky or Poole–Frenkel emission mechanism. The leakage current density at 1.0 V is equal to  $10^{-7}$  A/cm<sup>2</sup>. Since the conductivity is strongly affected by the characteristics of the film–electrode interface, the surface morphology of CCTO thin film is one of the major factors determining the leakage current in capacitors. The low leakage current value can be attributed to the small surface roughness as was observed by AFM in Fig. 3. No significant difference in leakage currents was observed when the bias was reversed. This is reasonable because the capacitor system is completely symmetrical, and CCTO do not show evidence of ferroelectric behavior. Thus, applying voltage in direction or the other will be totally equivalent, regardless of whether the conduction is limited by interfacial barriers or by bulk-like mechanisms.

It is well known that in most dielectric materials, the dielectric loss and leakage current density are related to the free carriers. The dielectric loss comes from two mechanisms [36]: the resistive loss and the relaxation loss of the dipole. In the resistive loss mechanism, the energy is consumed by free carriers in the film; while in the case of the relaxation loss mechanism, it is the relaxation of the dipole that expends energy. If there are free carriers in the films, the resistive loss is the dominant mechanism. Fig. 6 shows the variation of dielectric permittivity and dielectric loss as a function of frequency for the CCTO film. At 1 MHz, the dielectric permittivity and dielectric loss for the capacitor, was 1020 and 0.031, respectively. This value is different from that of the crystal, which is about 100 [3]. The large dielectric permittivity of CCTO has been interpreted as an extrinsic mechanism, which was assumed to come from the sample microstructure such as boundary or interface effects [37]. In fact, one recent paper has claimed that CCTO is a one-step internal barrier layer capacitor [5]. With such a model, one would conclude that the thin films have less defects than the crystals because of their lower dielectric permittivity. This is a possibility though it can often be the reverse. Thin films, with their much reduced size in one dimension, may have less planar defects, such as grain boundaries and twin interfaces, than crystals, particularly if the latter have a large amount of intrinsic planar defects. Finally, it is worth pointing out that the dielectric loss in the thin film is actually lower than in the crystal. This may well be a reflection that the crystals have more defects than the thin films being the dielectric permittivity in the thin film ( $\sim 1020$ ) much lower than in the crystal ( $\geq 10,000$ ). As it can be seen from Fig. 6, the dielectric permittivity shows very little dispersion with frequency indicating that the films possess low defect

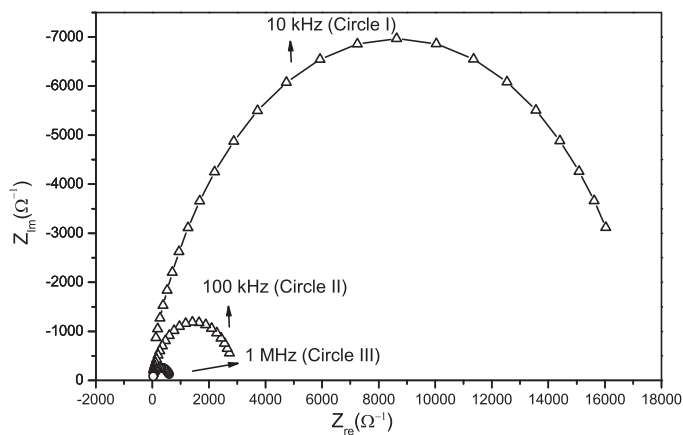
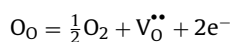


Fig. 7. Cole–Cole plot of complex-impedance diagram in the frequency range 100 Hz to 1 MHz for CCTO thin film deposited by the soft chemical method at 700 °C for 2 h in ambient atmosphere.

concentrations at the interface film–substrate. The low dispersion of the dielectric permittivity and the absence of any relaxation peak in  $\tan \delta$  indicate that an interfacial polarization of the Maxwell Wagner type and an interfacial polarization arisen from the electrode barrier are negligible in the film. The dielectric properties of the film obtained in the present work is comparable with that reported for polycrystalline CCTO thin films [10,38,8]. Dielectric permittivity as high as 2000 and dielectric loss of 0.05 has been reported for a polycrystalline CCTO thin film having 480 nm thickness produced by PLD [10]. Such improvement may be a result of the increased thickness, much closer package of uniform grains, crystal orientation and presence of buffer layer. Other explanation can be the presence of CuO based liquid phase sintering which increases the degree of disorder in the network forming positions with octahedral TiO<sub>6</sub> structural units. Such structural units may increase the rigidity of the network and cause to increase the values of dielectric parameters, as observed.

The complex impedance plane plot of  $Z'$  versus  $Z''$  (where  $Z'$  and  $Z''$  are the real and imaginary parts of the complex impedance, respectively) is used to understand the different relaxation processes as a consequence of different capacitive components. Impedance spectroscopic analysis was employed to verify the presence of intrinsic as well as the space-charge contributions to our measured values of the dielectric permittivity (Fig. 7). The Cole–Cole plot for the complex impedance in the 10 kHz to 1 MHz frequency range clearly reveals the presence of three overlapping semicircular arcs which are attributable to contributions from electrode–grain interface (circle I), grain boundary (circle II), and grains contribution (circle III) in the decreasing order of measuring frequencies [39–41]. The possible origin of different resistivities of grains and grain boundaries can be caused by the equilibrium concentration of oxygen vacancies in ABO<sub>3</sub> type perovskites which results in loss of oxygen during sintering. This loss can be written in the Kröger–Vink notation as follows:



The electrons released in the above reaction may be captured by Cu<sup>2+</sup> leading to the formation of Cu<sup>+</sup>. This leads to hopping of electrons among the two different valence states, which increases conductivity of the grains. During cooling down period after sintering, the reverse reaction occurs. However due to insufficient time available during cooling, the reoxidation occurs preferentially at grain boundaries only. Thus grain boundaries regain their insulating character, while the grains remain more or less semi-conducting. The grain boundaries thus act as barriers against the hopping electrons, which pile up against them leading to space

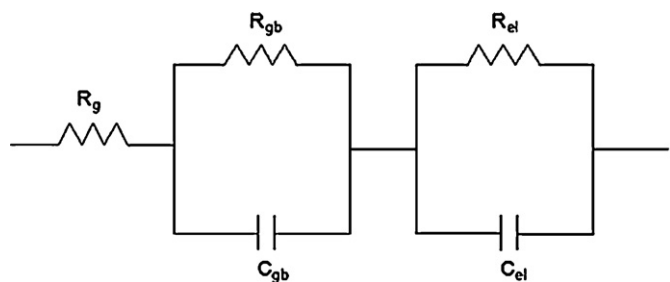


**Fig. 8.** Equivalent circuit model to describe the electrical properties of CCTO thin film deposited by the soft chemical method at 700 °C for 2 h in ambient atmosphere.

charge polarization. A similar space charge polarization occurs at the electrode–grain interface. These space charge polarization processes are responsible for the extremely large value of dielectric permittivity at very low and medium frequencies. Based on an equivalent circuit consisting of two parallel RC elements in series, the high frequency non-zero intercept indicates the presence of an arc with  $\omega\max$  greater than the highest frequency measured, which is assigned as the contribution from grain interior ( $R_g$ ), while the low frequency extrapolated intercept is attributed to the insulating grain boundaries ( $R_{gb}$ ). By assigning this equivalent circuit model, the CCTO film exhibited  $R_{gb}$  of  $\sim 2 \times 10^5$  and  $R_g$  of  $\sim 10 \Omega$ . The impedance parameters obtained in the present study is comparable with those reported for polycrystalline CCTO thin films [42,43]. Hence, the impedance spectroscopy studies revealed that the internal barrier layer effect, which depends upon the resistivity difference between the grain and grain boundary was pronounced in the CCTO film; thus giving a reasonable explanation for the higher  $k$  of the film. These results indicate that the grain and grain boundaries of CCTO film have different characteristics of electrical transport. Based on these observations, the CCTO film can be analyzed using the equivalent circuit consisting of a resistor connected in series with two resistor–capacitor (RC) elements as shown in Fig. 8, element  $R_g$  representing the grain,  $R_{gb}C_{gb}$  representing the grain boundary and  $R_{el}C_{el}$  representing the electrode–sample interface. Where  $R_g$  is the grain resistance,  $R_{gb}$ ,  $R_{el}$  and  $C_{gb}$ ,  $C_{el}$  are the resistance and capacitance associated with the grain boundary and the electrode–sample interface, respectively.

#### 4. Conclusions

Good quality polycrystalline CCTO thin film was prepared by the soft chemical method at a substrate temperature of 700 °C for 2 h. The XRD studies revealed the polycrystalline nature of the film belonging to the  $Im-3$  space group. The film exhibited a duplex microstructure consisting of large and fine grains. Raman analyses reveal active normal modes of the minority phases CuO and TiO<sub>2</sub> and the main modes of the structural CCTO phase. The 250 nm film had a high dielectric constant of 1020 at 1 MHz. Leakage measurements do not show any evidence of ferroelectric behavior, regardless of whether the conduction is limited by interfacial barriers or by bulk-like mechanisms. Based on impedance analyses, the grain and grain boundaries of this material have different characteristics of electrical transport. The high value found for the high frequency dielectric constant makes the sol–gel prepared CCTO thin films good candidates for DRAM applications.

#### Acknowledgments

The financial support of this research project by the Brazilian research funding agencies CNPq and FAPESP is gratefully acknowledged.

#### References

- [1] M.A. Subramanian, D. Li, N. Duan, B.A. Reisner, A.W. Sleight, J. Solid State Chem. 151 (2000) 323–325.
- [2] D. Szwagierczak, J. Kulawik, J. Alloys Compd. 491 (2010) 465–471.
- [3] C.M. Wang, L. Shih-Yuan, K.S. Kao, Y.C. Chen, S.C. Weng, J. Alloys Compd. 491 (2010) 423–430.
- [4] L. Ramajo, R. Parra, J.A. Varela, M.M. Reboredo, M.A. Ramirez, M.S. Castro, J. Alloys Compd. 497 (2010) 349–353.
- [5] R. Parra, R. Savu, L.A. Ramajo, M.A. Ponce, J.A. Varela, M.S. Castro, P.R. Bueno, E. Joanni, J. Solid State Chem. 183 (2010) 1209–1214.
- [6] C. Kant, T. Rudolf, S. Drohns, P. Lukenheimer, S.G. Ebbinhaus, A. Loidl, Phys. Rev. B 77 (2008) 045131–045134.
- [7] S.F. Shao, J.L. Zhang, P. Zheng, C.L. Wang, Solid State Commun. 142 (2007) 281–286.
- [8] M.-H. Wangbo, M.A. Subramanian, Chem. Mater. 18 (2006) 3257–3260.
- [9] J. Li, A.W. Sleight, M.A. Subramanian, Solid State Commun. 135 (2005) 260–263.
- [10] M.J. Pan, B.A. Bender, J. Am. Ceram. Soc. 88 (2005) 2611–2614.
- [11] L. Fang, M. Shen, W. Cao, J. Appl. Phys. 95 (2004) 6483–6485.
- [12] L. Wu, Y. Zhu, S. Park, S. Shapiro, G. Shirane, Phys. Rev. B 71 (2005) 014118–014121.
- [13] V. Brizé, G. Gruener, J. Wolfman, K. Fatyeyeva, M. Tabellout, M. Gervais, Mater. Sci. Eng. B 129 (2006) 135–138.
- [14] P. Leret, J.F. Fernandez, J. de Frutos, D. Fernandez-Hevia, J. Eur. Ceram. Soc. 27 (2007) 3901–3905.
- [15] S.-Y. Chung, I.-D. Kim, S.-J.L. Kang, Nat. Mater. 3 (2004) 774–778.
- [16] L. Fang, M. Shen, D. Yao, Appl. Phys. A 80 (2005) 1763–1767.
- [17] L. Fang, M. Shen, Thin Solid Films 440 (2003) 60–63.
- [18] J.A. Bermudez, M.Sc. thesis, Universidad de Puerto Rico, 2004.
- [19] W. Lu, L. Feng, G. Cao, Z. Jiao, Mater. Sci. 39 (2004) 3523–3524.
- [20] A.Z. Simões, B.D. Stojanovic, A. Tangastev, N. Setter, J.A. Varela, Integr. Ferroelectr. 43 (2002) 123–125.
- [21] A.Z. Simões, A. Ries, F.M. Filho, J.A. Varela, E. Longo, Appl. Phys. Lett. 85 (2004) 5962–5964.
- [22] A.Z. Simões, L.S. Cavalcante, C.S. Riccardi, J.A. Varela, E. Longo, Curr. Appl. Phys. 9 (2009) 502–523.
- [23] A.Z. Simões, E.C. Aguiar, E. Longo, J.A. Varela, Mater. Chem. Phys. 115 (2009) 434–438.
- [24] S.B. Desu, H.S. Cho, P.C. Joshi, Appl. Phys. Lett. 70 (1997) 1393–1395.
- [25] E.R. Leite, C.M.G. Campos, E. Longo, J.A. Varela, Ceram. Int. 21 (1995) 143–152.
- [26] D. Laudisio, M. Catauro, A. Aronne, P. Pernice, Thermochim. Acta 94 (1997) 173.
- [27] H.-F. Wu, C.-C. Lin, P. Shen, J. Non-Cryst. Solids 209 (1997) 76.
- [28] G. Murali Krishna, N. Veeraiah, N. Venkatramaiah, R. Venkatesan, J. Alloys Compd. 450 (2008) 477–485.
- [29] A.F.L. Almeida, R.E.S. Oliveira, J.M. Sasaki, A.S.B. Sombra, L.C. Kretly, Microw. Opt. Technol. Lett. 39 (2003) 145–150.
- [30] J.F. Xu, W. Ji, Z.X. Shen, W.S. Li, S.H. Tang, X.R. Ye, D.Z. Jia, X.Q. Xin, J. Raman Spectrosc. 30 (1999) 413–415.
- [31] L. He, J.B. Neaton, M.H. Cohen, D. Vanderbilt, Phys. Rev. B 65 (2002) 214112–214122.
- [32] M. Pineda, J.L.G. Fierro, J.M. Palacios, C. Silleruelo, E. Garcia, J.V. Ibarra, Appl. Surf. Sci. 119 (1997) 1–10.
- [33] F. Amaral, C.P.L. Rubinger, M.A. Valente, L.C. Costa, R.L. Moreira, J. Appl. Phys. 105 (2009) 034109–034114.
- [34] B.V. Raghavaiah, C. Laxmikanth, N. Veeraiah, Opt. Commun. 235 (2004) 341–349.
- [35] L. Srinivasa Rao, M. Srinivasa Reddy, D. Krishna Rao, N. Veeraiah, Solid State Sciences 11 (2009) 578–587.
- [36] P. Li, J.F. McDonald, T.M. Lu, J. Appl. Phys. 71 (1992) 5596–5600.
- [37] L. He, J.B. Neaton, M.H. Cohen, D. Vanderbilt, C.C. Homes, Phys. Rev. B 65 (2002) 214112–214115.
- [38] W. Si, E.M. Cruz, P.D. Johnson, P.W. Barnes, P. Woodward, A.P. Ramirez, Appl. Phys. Lett. 81 (2002) 2056–2058.
- [39] T. Kanai, S.I. Ohkoshi, K. Hashimoto, J. Phys. Chem. Solids 64 (2003) 391–397.
- [40] T. Kojima, T. Sakai, T. Watanabe, H. Funakubo, Appl. Phys. Lett. 80 (2002) 2746–2748.
- [41] A.K. Joncher, Dielectric Relaxation in Solids, Chelser Dielectric, London, 1983.
- [42] L. Fang, M. Shen, Z. Li, W. Cao, Chin. Phys. Lett. 23 (2006) 990–993.
- [43] B. Shri Prakash, K.B.R. Varma, D. Michau, M. Maglione, Thin Solid Films 516 (2008) 2874–2877.